Multicomponent Reactive Dispersion in Tubes: Collocation vs. Radial Averaging

Orthogonal collocation is used to analyze the dispersion and chemical conversion of a multicomponent fluid pulse in a laminar isothermal flow in a catalytic tube. Homogeneous and heterogeneous first-order chemical reactions are included, and a full matrix diffusion law is used. The collocation method represents the dynamics well over wide ranges of system parameters and reaction time. Radial averaging approaches prove less convenient, since the dispersion coefficients thus introduced are complicated functions of time, transport properties and chemical kinetics.

J. Chih Wang
Warren E. Stewart
Chemical Engineering Department
University of Wisconsin
Madison, WI 53706

Introduction

Dispersion effects are widely encountered in chemical reactors and mass transfer systems. In process models, such systems are often treated as one-dimensional by use of transversely averaged mass and energy balances. The local velocity and thermodynamic state in such a model stand for averages over a cross-section of the flow, and the convective dispersion (caused by deviations from these averages) is modelled as enhanced longitudinal diffusion and conduction.

The transverse-average approach has been developed extensively for laminar flows in tubes. Taylor (1953) and Aris (1956) derived radially averaged formulas from the long-time asymptotes of their two-dimensional problems. Gill and Sankarasubramanian (1970, 1973, 1974) introduced a set of time-dependent dispersion coefficients $K_i(t)$, and treated first-order reacting systems. DeGance and Johns (1978, 1979) gave more detailed transient solutions, using a new set of dispersion coefficients $X_i(t)$ based on axial moments of the solute concentration. Multicomponent reacting systems have been studied by DeGance and Johns (1980, 1985, 1987), Aris (1980), and Hatton (1981), but only partial results have been obtained.

Transversely averaged equations have limited predictive power, since the dispersion coefficients vary with time and with the form of the given problem. The long-time asymptotic forms of these equations are simpler, but also less useful in the presence of fast surface reactions (Aris, 1980). For predictive purposes, an efficient simulation of the process in its full set of dimensions should be preferred. We demonstrate and test the latter approach here, extending the collocation scheme of Wang and Stewart (1983) to reactive multicomponent systems.

Present address of J. C. Wang: Rohm & Haas Research, Bristol, PA 19007.

Problem Statement

A multicomponent stream in steady, developed flow through a tube is initially in chemical equilibrium at a uniform composition ω_0. At time $\tau = 0$ a small mass of miscible fluid is injected. The resulting mass-fraction disturbance vector, $\Delta\omega = \omega - \omega_0$, of dimension N is described by the mass-balance equation

$$\frac{\partial \Delta\omega}{\partial \tau} + V(\xi)\frac{\partial \Delta\omega}{\partial Z} = \boldsymbol{D}^{(N)}\left[\frac{1}{\xi}\frac{\partial}{\partial \xi}\left(\xi\frac{\partial \Delta\omega}{\partial \xi}\right) + \frac{1}{Pe^2}\frac{\partial^2 \Delta\omega}{\partial Z^2}\right] - \boldsymbol{K}'''\Delta\omega \quad (1)$$

with the boundary conditions

$$\frac{\partial \Delta\omega}{\partial \xi} = \boldsymbol{0} \quad \text{at} \quad \xi = 0 \quad (2)$$

$$\boldsymbol{D}^{(N)}\frac{\partial \Delta\omega}{\partial \xi} + \boldsymbol{K}''\Delta\omega = \boldsymbol{0} \quad \text{at} \quad \xi = 1 \quad (3)$$

and the initial pulse distribution

$$\Delta\omega = \Gamma(\xi, Z) \quad \text{at} \quad \tau = 0_+ \quad (4)$$

To bound the solutions, we require that the pulse have bounded mass of each constituent, and that Γ be negligible outside some finite interval $[-Z_0, +Z_0]$.

The system is treated as isothermal, with constant density and constant matrices $\boldsymbol{D}^{(N)}$, $\boldsymbol{K}''$ and $\boldsymbol{K}'''$ of order N. Interfacial accumulation is neglected according to Eq. 3. All quantities in these equations are dimensionless; in particular, $\boldsymbol{D}^{(N)}$ is the diffusivity matrix $[\mathcal{D}]$ divided by its greatest absolute element, $\mathcal{D}_{ref}$, and ξ is

the radial cylindrical coordinate normalized to unity at the wall.

Equations 1–4 are written for a vector $\Delta\omega$ of minimum dimension N, just sufficient to determine the mass fractions of the remaining species. That is, the included species, $1, \ldots N$ are selected to provide a basis of mass-fraction displacements $\Delta\omega_1, \ldots \Delta\omega_N$.

The Poiseuille velocity function, $1 - \xi^2$, is used in our numerical examples, but in the rest of this work a flexible V-profile is used. Our procedures hold directly for other developed velocity distributions $V(\xi)$, such as those of non-Newtonian flows.

Collocation

An approximate solution for $\Delta\omega$ is sought by orthogonal collocation (Villadsen and Stewart, 1967; Stewart, 1984). The vector $\Delta\omega$ in Eqs. 1–4 is approximated by the function

$$\Delta\tilde{\omega} = \sum_{j=1}^{n+1} \ell_j(\xi^2)\Delta\tilde{\omega}(\tau, \xi_j, Z) \tag{5}$$

set up by Lagrangian interpolation in ξ^2. The collocation nodes $\xi_1, \ldots \xi_n$ within the tube are chosen as the positive zeros of the Legendre polynomial $P_{2n}(\xi)$, and the node ξ_{n+1} is placed at the wall as in Wang and Stewart (1983). The collocation is then performed by making $\Delta\tilde{\omega}$ satisfy Eqs. 1, 3 and 4 on the relevant nodes. Equation 2 is satisfied directly by $\Delta\tilde{\omega}$ since only even powers of ξ appear in Eq. 5.

Application of Eq. 1 to the approximant $\Delta\tilde{\omega}$ at each interior node ξ_i gives the differential equation system

$$\frac{\partial\Delta\tilde{\omega}_i}{\partial\tau} + V(\xi_i)\frac{\partial\Delta\tilde{\omega}_i}{\partial Z} = \boldsymbol{D}^{(N)}\sum_{j=1}^{n+1} B_{ij}\Delta\tilde{\omega}_j + \frac{1}{Pe^2}\boldsymbol{D}^{(N)}\frac{\partial^2\Delta\tilde{\omega}_i}{\partial Z^2} - \boldsymbol{K}'''\Delta\tilde{\omega}_i \quad i = 1, \ldots n \tag{6}$$

Here $\Delta\tilde{\omega}_k$ denotes the N-vector $\Delta\tilde{\omega}(\tau, \xi_k, Z)$, and B_{ij} is the Laplacian of $\ell_j(\xi^2)$ at ξ_i. Application of Eq. 3 to $\Delta\tilde{\omega}$ gives the difference equation system

$$\boldsymbol{D}^{(N)}\sum_{j=1}^{n+1} A_{n+1,j}\Delta\tilde{\omega}_j + \boldsymbol{K}''\Delta\tilde{\omega}_{n+1} = \boldsymbol{0} \tag{7}$$

in which $A_{n+1,j}$ denotes $d\ell_j(\xi^2)/d\xi$ evaluated at ξ_{n+1}. Elimination of the interfacial state $\Delta\tilde{\omega}_{n+1}$ from Eq. 6 by use of Eq. 7 gives a modified differential system, expressible in partitioned matrix form as

$$\begin{bmatrix} \frac{\partial\Delta\tilde{\omega}_1}{\partial\tau} \\ \vdots \\ \frac{\partial\Delta\tilde{\omega}_n}{\partial\tau} \end{bmatrix} + \begin{bmatrix} V(\xi_1)\boldsymbol{I} & & \boldsymbol{0} \\ & \ddots & \\ \boldsymbol{0} & & V(\xi_n)\boldsymbol{I} \end{bmatrix} \begin{bmatrix} \frac{\partial\Delta\tilde{\omega}_1}{\partial Z} \\ \vdots \\ \frac{\partial\Delta\tilde{\omega}_n}{\partial Z} \end{bmatrix} = \begin{bmatrix} \boldsymbol{J}_{11} - \boldsymbol{K}''', \boldsymbol{J}_{12}, \ldots \boldsymbol{J}_{1n} \\ \boldsymbol{J}_{21}, \quad \ddots \\ \vdots \\ \boldsymbol{J}_{n1}, \ldots \quad \boldsymbol{J}_{nn} - \boldsymbol{K}''' \end{bmatrix} \begin{bmatrix} \Delta\tilde{\omega}_1 \\ \vdots \\ \Delta\tilde{\omega}_n \end{bmatrix}$$

$$+ \frac{1}{Pe^2}\begin{bmatrix} \boldsymbol{D}^{(N)} & & \boldsymbol{0} \\ & \ddots & \\ \boldsymbol{0} & & \boldsymbol{D}^{(N)} \end{bmatrix} \begin{bmatrix} \frac{\partial^2\Delta\tilde{\omega}_1}{\partial Z^2} \\ \vdots \\ \frac{\partial^2\Delta\tilde{\omega}_n}{\partial Z^2} \end{bmatrix} \tag{8}$$

The submatrices $\boldsymbol{J}_{ij}$ are given by

$$\boldsymbol{J}_{ij} = B_{ij}\boldsymbol{D}^{(N)} - B_{i,n+1}A_{n+1,j}\boldsymbol{D}^{(N)}(\boldsymbol{K}'' + A_{n+1,n+1}\boldsymbol{D}^{(N)})^{-1}\boldsymbol{D}^{(N)} \quad \begin{Bmatrix} i = 1, \ldots, n \\ j = 1, \ldots, n \end{Bmatrix} \tag{9}$$

in which the inversion is unique at locally stable states as shown in Appendix B. The weights $A_{n+1,j}$ and B_{ij}, as well as the nodes ξ_j, are computable via the algorithms of Villadsen and Michelsen (1978).

For conciseness, we define the interior solution vector

$$\boldsymbol{\Omega} = \begin{bmatrix} \Delta\tilde{\omega}_1 \\ \vdots \\ \Delta\tilde{\omega}_n \end{bmatrix} \tag{10}$$

and correspondingly abbreviate Eq. 8:

$$\frac{\partial\boldsymbol{\Omega}}{\partial\tau} + \boldsymbol{V}\frac{\partial\boldsymbol{\Omega}}{\partial Z} = \boldsymbol{B}''\boldsymbol{\Omega} + \frac{1}{Pe^2}\boldsymbol{D}\frac{\partial^2\boldsymbol{\Omega}}{\partial Z^2} \tag{11}$$

Equation 4 then takes the radially discretized form,

$$\boldsymbol{\Omega} = \begin{bmatrix} \Gamma(\xi_1, Z) \\ \vdots \\ \Gamma(\xi_n, Z) \end{bmatrix} \quad \text{at} \quad \tau = 0_+ \tag{12}$$

various cases of which are analyzed below.

This completes the restatement of Eqs. 1–4 as a collocation problem. Nonlinear problems can be handled similarly. Thus, nonlinear kinetics would be handled by revising the reaction rate functions in Eqs. 6 and 7. Numerical solution procedures then would normally be required.

Concentration Profiles for Binary Reaction Systems

Equations 11 and 12 can be solved analytically with two interior nodes ($n = 2$), for binary systems ($N = 1$) without axial diffusion. For a pulse initially localized at $Z = 0$, with a radial mass distribution $Q(\xi)$, the function Γ in Eq. 4 is $Q(\xi)\delta(Z)$. The resulting nodal solutions are

$$\Omega_{1\infty} = \left\{\frac{Q_1\beta I_1(X)|T + Z_s|}{2X} + \frac{Q_2 B''_{12} I_0(X)}{|V_1 - V_2|} + Q_1\delta(Z_s - T)\right\}e^{\alpha} \tag{13}$$

$$\Omega_{2\infty} = \left\{ \frac{Q_2 \beta I_1(X) |T - Z_s|}{2X} + \frac{Q_1 B''_{21} I_0(X)}{|V_1 - V_2|} + Q_2 \delta(Z_s + T) \right\} e^{\alpha} \tag{14}$$

for $Z_s^2 \leq T^2$, and vanish identically outside this region. Here

$$Z_s = Z - (V_1 + V_2)\tau/2 \tag{15}$$

$$T = (V_1 - V_2)\tau/2 \tag{16}$$

$$\beta = 4B''_{12}B''_{21}(V_1 - V_2)^{-2} \tag{17}$$

$$X = \sqrt{\beta(T^2 - Z_s^2)} \tag{18}$$

$$\alpha = \left(\frac{B''_{11} + B''_{22}}{2} \right) \tau + \frac{(B''_{11} - B''_{22}) Z_s}{V_1 - V_2}, \tag{19}$$

V_i and Q_i are the nodal values of velocity $V(\xi)$ and initial radial distribution $Q(\xi)$, and the elements B''_{ij} are given by

$$B''_{11} = -K''' + 12[(4/\sqrt{3} - 3)K''^2 + (8/\sqrt{3} - 14)K'' - 16]/(K''^2 + 14K'' + 24) \tag{20}$$

$$B''_{22} = -K''' - 12[(3 + 4/\sqrt{3})K''^2 + (8/\sqrt{3} + 14)K'' + 16]/(K''^2 + 14K'' + 24) \tag{21}$$

$$B''_{12} = B''_{21} = 12(K''^2 + 10K'' + 16)/(K''^2 + 14K'' + 24) \tag{22}$$

Non-parabolic velocity functions $V(\xi)$ are permitted in this solution, as long as V_1 and V_2 are unequal.

Equations 13 and 14 have a smooth central region $Z_s^2 < T^2$, bordered by spikes (δ-functions) at $Z_s^2 = T^2$ and by undisturbed upstream and downstream regions $Z_s^2 > T^2$. The spikes, moving at the nodal fluid velocities, are remnants of the initial sharp pulse; they transform to Gaussian distributions when these solutions are corrected as below for longitudinal molecular diffusion.

Tests of Binary Concentration Profiles

As a test of the two-point solution just given, we calculate the evolution of a nearly rectangular pulse of unit height and of length L equal to 0.1 unit of Z, for a binary system with a first-order irreversible wall reaction. The original composition is reactant-free; hence $\Delta\omega = \omega$ for the reactant species.

A reference solution ω_∞ with $Pe \rightarrow \infty$ (no axial diffusion) is first computed. The region accessible to the injected solute in this case extends from $Z = -L/2$ to $Z = L/2 + \tau$. A stretched axial coordinate,

$$U = (2Z - \tau)/(L + \tau) \tag{23}$$

is introduced in Eqs. 11 and 12 so that the disturbance region for ω_∞ extends from $U = -1$ to $U = 1$ for all $\tau > 0$.

The chosen initial pulse distribution is radially uniform; thus

$$\text{At} \quad \tau = 0_+, \quad \Delta\omega = \Gamma(\xi, Z) = g(U) \tag{24}$$

A nearly rectangular, but differentiable g-profile is used:

$$g(U) = 1 \quad \text{for} \quad |U| \leq 0.975 \tag{25}$$

$$g(U) = 1 - 3\left[\frac{|U| - 0.975}{0.025}\right]^2 + 2\left[\frac{|U| - 0.975}{0.025}\right]^3 \quad \text{for } 0.975 < |U| < 1 \tag{26}$$

$$g(U) = 0 \quad \text{for} \quad |U| \geq 1 \tag{27}$$

This function has C^1 continuity (continuous g and dg/dU), consistent with the basis functions used in the finite-element integration of Eq. 11.

Figures 1, 2 and 3 show the cross-sectional average reactant concentration profiles for surface Damköhler numbers $K'' = 0.1$, 1 and 10. These values at $Pe = 40$ are derived, by the convolution formula of Wang and Stewart (1983), from various

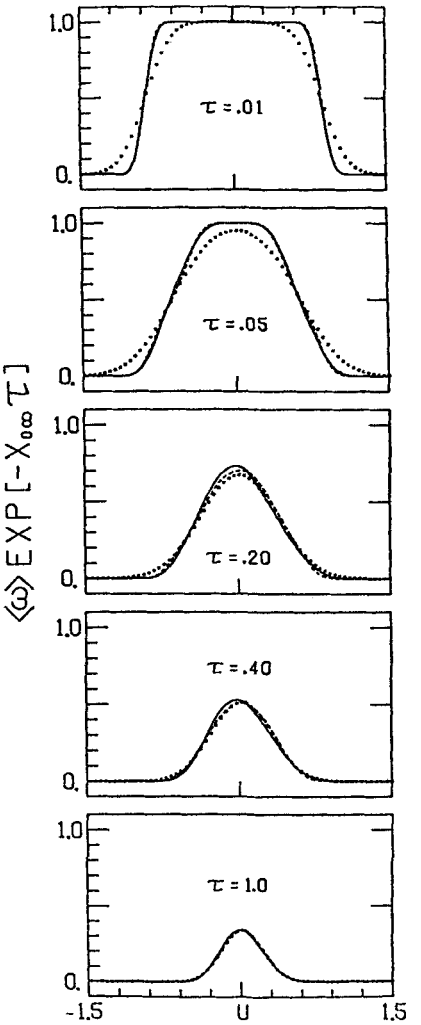

Figure 1. Cross-sectional area average compositions in a binary system with $Pe = 40$, $K''' = 0$, and $K'' = 0.1$.

— reference solution by finite elements
---- collocation with two radial nodes
**** constant-coefficient version of generalized dispersion theory

approximations to the infinite-*Pe* solution:

i) Fine-grid collocation on cylindrical finite elements, with temporal integration by the subroutine package EPISODE of Hindmarsh and Byrne (1975)

ii) Superposition of the two-point radial collocation results in Eqs. 13–14 to match the initial distribution $g(U)$

iii) The constant-coefficient version of a radially averaged dispersion model (DeGance and Johns, 1978).

The finite elements for method (i) were cylinders, $\xi^2 \leq 1$, of length $\Delta U = 0.025$. Collocation on these elements, with quartic polynomials in ξ^2 and C^1 cubic splines in U, gave a (4×2)-point interior grid for each of the 40 elements. For readability, in Figures 1–3 the mass fractions for all methods are divided by exp $[X_{0\infty}\tau]$. The latter function is the unconverted reactant fraction predicted by the radially averaged model, and is represented by the broken lines in Figure 4.

The two-point collocation values in Figures 1–3 (dashed curves) closely approximate the fine-grid computations, except for long times at the largest K'' (see Figure 3) where the division by exp $[X_{0\infty}\tau]$ significantly magnifies the deviations. The constant-coefficient, radially averaged model is less accurate at short times, particularly when the heterogeneous reaction is fast. The variable-coefficient dispersion theory of Sankarasubramanian and Gill (1973, 1974) (not plotted because of crowding) gives results quite comparable here to the two-point collocation values.

Axial Moments of the Concentration Profiles

Equations 11 and 12 require numeric treatment for finer grids ($n > 2$), and for multicomponent dispersion ($N \geq 2$, $n \geq 2$). However, their axial moments remain solvable analytically. Consider the moment vectors

$$M_i(\tau) = \int_{-\infty}^{\infty} Z^i \Omega(\tau) dZ \quad i = 0, 1, 2, \ldots \tag{28}$$

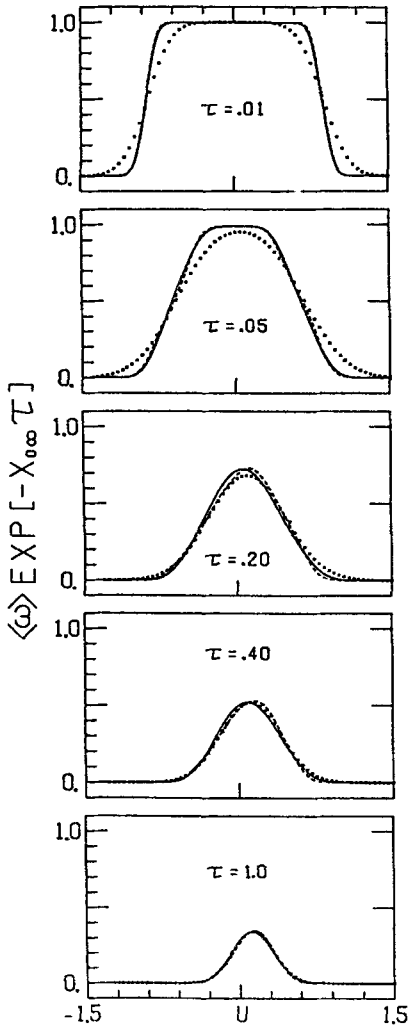

Figure 2. Cross-sectional area average compositions in a binary system with *Pe* = 40, *K'''* = 0, and *K''* = 1.0.

— reference solution by finite elements
---- collocation with two radial nodes
**** constant-coefficient version of generalized dispersion theory

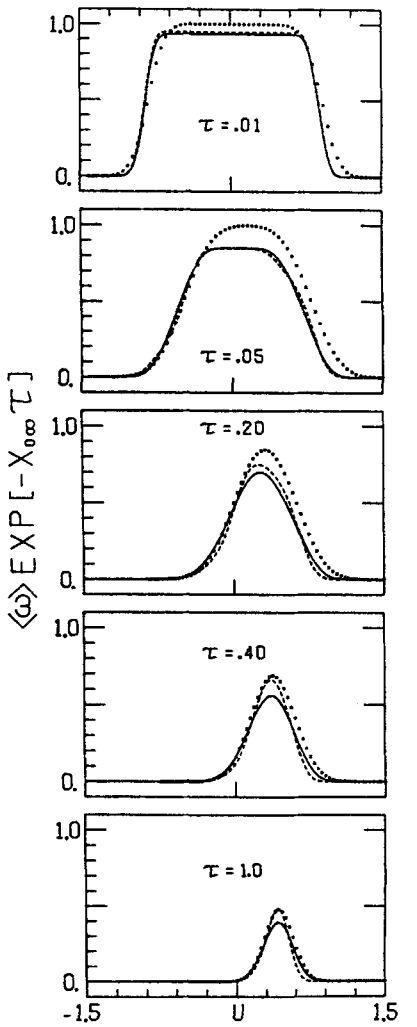

Figure 3. Cross-sectional area average compositions in a binary system with *Pe* = 40, *K'''* = 0, and *K''* = 10.

— reference solution by finite elements
---- collocation with two radial nodes
**** constant-coefficient version of generalized dispersion theory

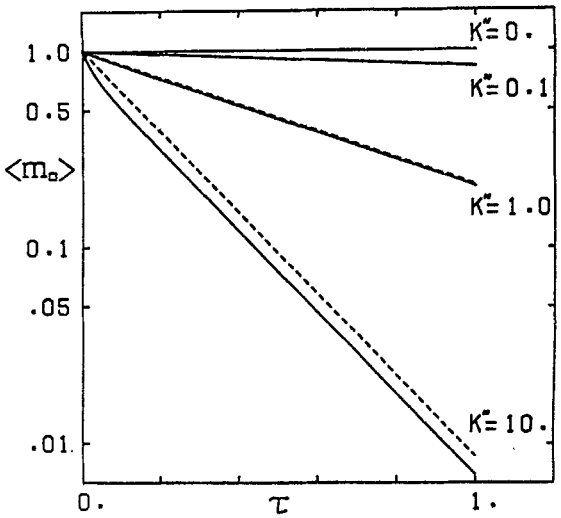

Figure 4. Time dependence of remaining reactant mass in a binary system with a wall reaction.
— collocation with $n \geq 2$ radial nodes
---- constant-coefficient version of generalized dispersion theory

and their generating function

$$M_i(\tau) = \left(-\frac{d}{dp}\right)^i [\bar{\Omega}(\tau, p)]_{p=0} \tag{29}$$

in which $\bar{\Omega}(\tau, p)$ is the Fourier transform (Campbell and Foster, 1967) of $\Omega(\tau, Z)$. Taking the Fourier transforms of Eqs. 11 and 12, and inserting Eq. 29, we obtain the moment equations

$$\frac{dM_i}{d\tau} = B''M_i + iVM_{i-1} + \frac{i(i-1)}{Pe^2} DM_{i-2} \tag{30}$$

$$M_i = M_i(0) \quad \text{at} \quad \tau = 0_+ \tag{31}$$

which are solvable sequentially by matrix calculus. The results for the first three moments are:

$$M_0 = P \exp(\lambda\tau) P^{-1} M_0(0) \tag{32}$$

$$M_1 = P \exp(\lambda\tau) P^{-1} M_1(0) + PQP^{-1} M_0(0) \tag{33}$$

$$M_2 = P \exp(\lambda\tau) P^{-1} M_2(0) + 2PQP^{-1} M_1(0) + 2PRP^{-1} M_0(0) + \frac{2}{Pe^2} PQ^{\sharp} P^{-1} M_0(0) \tag{34}$$

Here λ is the diagonal matrix of eigenvalues (assumed distinct) of the matrix B'', and P is the corresponding matrix of column eigenvectors. The elements of the matrices Q and R are

$$Q_{ii} = F_{ii}\tau \exp(\lambda_i\tau) \tag{35}$$

$$Q_{ij} = F_{ij}[\exp(\lambda_i\tau) - \exp(\lambda_j\tau)]/(\lambda_i - \lambda_j) \qquad i \neq j \tag{36}$$

$$R_{ii} = \frac{1}{2} F_{ii}^2 \tau^2 e^{\lambda_i\tau} + \sum_{\substack{k=1 \\ k\neq i}}^{nN} F_{ik}F_{ki}\left[\frac{\tau e^{\lambda_i\tau}}{\lambda_i - \lambda_k} + \frac{e^{\lambda_k\tau} - e^{\lambda_i\tau}}{(\lambda_i - \lambda_k)^2}\right] \tag{37}$$

$$R_{ij} = F_{ij}F_{jj}\left[\frac{\tau e^{\lambda_j\tau}}{\lambda_j - \lambda_i} - \frac{e^{\lambda_j\tau} - e^{\lambda_i\tau}}{(\lambda_j - \lambda_i)^2}\right] - \frac{F_{ii}F_{ij}\tau e^{\lambda_i\tau}}{\lambda_j - \lambda_i} + \sum_{\substack{k=1 \\ k\neq j}}^{nN} \cdot \frac{F_{ik}F_{kj}(e^{\lambda_j\tau} - e^{\lambda_i\tau})}{(\lambda_j - \lambda_k)(\lambda_j - \lambda_i)} + \sum_{\substack{k=1 \\ k\neq i,j}}^{nN} \frac{F_{ik}F_{kj}(e^{\lambda_k\tau} - e^{\lambda_i\tau})}{(\lambda_j - \lambda_k)(\lambda_i - \lambda_j)}, \quad i \neq j \tag{38}$$

in which the elements $F_{ii}, F_{ij}, \ldots$ come from the matrix

$$F = P^{-1}VP \tag{39}$$

The matrix $Q^{\sharp}$ in Eq. 34 is constructed like Q except for replacement of F by the matrix

$$F^{\sharp} = P^{-1} \operatorname{diag}\{D^{(N)}, \ldots D^{(N)}\}P = P^{-1}DP \tag{40}$$

Higher moments $M_i(\tau)$ can be calculated by recursion as described in Appendix A.

Our computations for reactive systems have consistently given real, negative eigenvalues $\lambda_1, \ldots \lambda_{nN}$. This behavior is consistent with the properties proved in Appendix B for the radial operator T, of which the matrix B'' is a finite-dimensional approximation. The eigenvalues of T are shown there to be nonpositive, and to include a zero if the kinetic scheme has more than one equilibrium solution.

These moment solutions could be combined with laboratory data to evaluate rate constants and transport coefficients in Eqs. 1 and 3. The moments could also be used in principle to calculate the concentration field, though experience suggests that this will not be easy.

Multicomponent Dispersion Coefficients

For a multicomponent system, the dispersion coefficients are matrices $X_k(\tau)$ of order N, defined by the moment equations

$$\frac{d}{d\tau}\langle Wm_i\rangle = \sum_{k=0}^{i} X_k \langle Wm_{i-k}\rangle \qquad i = 0, 1, 2, \ldots \tag{41}$$

Here radially continuous moment vectors are used,

$$m_i = \int_{-\infty}^{\infty} Z^i \Delta\omega(\tau, \xi, Z)\, dZ \tag{42}$$

and $W(\xi)$ is a matrix of weighting functions. The definition is unique for a given radial weighting, provided that the matrix of weighted moments $\{\langle Wm_{i-k}\rangle;\ k \leq i\}$ is nonsingular. Definitions consistent with Eq. 41 are used by Hatton and Lightfoot (1984) and by DeGance and Johns (1985, 1987).

The dispersion coefficients X_i depend on τ and on the initial

Table 1. Long-Time Asymptotic Values of $-(K''' + X_{0\infty})$

K''	Approx. by Radial Collocation $n = 2$	$n = 3$	$n = 4$	Analytic Values*
0	0	0	0	0
0.1	0.1951	0.1951	0.1951	0.1951
1.0	1.5770	1.5770	1.5770	1.5770
10.0	4.7562	4.7502	4.7502	4.7502
∞	5.8007	5.7832	5.7832	5.7832

*From Eq. 33 of Sankarasubramanian and Gill (1973) or Eq. 21 of DeGance and Johns (1978); the first four values are from Aris (1980).

Table 2. Long-Time Asymptotic Values of $X_{1\infty}$

K''	Approx. by Radial Collocation $n=2$	$n=3$	$n=4$	Analytic Values*
0	0.5	0.5	0.5	0.5
0.1	0.5082	0.5082	0.5082	0.5082
1.0	0.5717	0.5720	0.5720	0.5720
10.0	0.7277	0.7370	0.7370	0.7370
∞	0.7649	0.7818	0.7819	0.7819

*From Eq. 53 of Sankarasubramanian and Gill (1973) or Eq. 22 of DeGance and Johns (1978); numerical values are from Aris (1980).

pulse distribution $\Gamma(Z, \xi)$, as well as on the matrices $\boldsymbol{D}^{(N)}$, $\boldsymbol{K}''$ and $\boldsymbol{K}'''$. Here we consider only the long-time asymptotes $\boldsymbol{X}_{i\infty}$, which give a "constant-coefficient" dispersion model when used in Eq. 41.

The solutions $\boldsymbol{M}_k(\tau)$ in the previous section provide collocation solutions for the interpolated moments $\tilde{\boldsymbol{m}}_k(\xi, \tau)$, at the nodes of an n-point Gaussian quadrature over the interval $0 < \xi^2 < 1$. Thus, the transverse averages in Eq. 41 can be expressed by quadrature as

$$\langle \boldsymbol{W}\tilde{\boldsymbol{m}}_k \rangle \doteq \boldsymbol{H}\boldsymbol{M}_k \tag{43}$$

in which $\boldsymbol{H}$ is the $N \times nN$ matrix

$$\boldsymbol{H} = [w_1\boldsymbol{W}(\xi_1) \ldots w_n\boldsymbol{W}(\xi_n)]/(w_1 + \cdots + w_n) \tag{44}$$

and $w_1, \ldots w_n$ are the Gaussian quadrature weights. Equation 43 integrates the functions $\boldsymbol{W}(\xi)\tilde{\boldsymbol{m}}_k(\xi, \tau)$ exactly if each element of $\boldsymbol{W}(\xi)$ is a linear combination of even functions $\xi^0, \ldots, \xi^{2n-4}$.

In the long-time limit, the functions $\boldsymbol{H}\boldsymbol{M}_k$ are dominated by the largest eigenfunctions in the $\boldsymbol{M}_k(\tau)$ solutions. Accordingly truncating Eqs. 32–34 and using Eq. 43, we obtain the following long-term asymptotes for the matrices $\boldsymbol{X}_k$:

$$\boldsymbol{X}_{0\infty} = \boldsymbol{H}\boldsymbol{P}_I\boldsymbol{\lambda}_I(\boldsymbol{H}\boldsymbol{P}_I)^{-1} \tag{45}$$

$$\boldsymbol{X}_{1\infty} = \boldsymbol{H}\boldsymbol{P}_I\boldsymbol{F}_D(\boldsymbol{H}\boldsymbol{P}_I)^{-1} + \boldsymbol{H}\boldsymbol{P}\boldsymbol{S}_I(\boldsymbol{H}\boldsymbol{P}_I)^{-1}\boldsymbol{X}_{0\infty} - \boldsymbol{X}_{0\infty}\boldsymbol{H}\boldsymbol{P}\boldsymbol{S}_I(\boldsymbol{H}\boldsymbol{P}_I)^{-1} \tag{46}$$

$$\boldsymbol{X}_{2\infty} = \boldsymbol{H}\boldsymbol{P}_I(\boldsymbol{F}\boldsymbol{S})_D(\boldsymbol{H}\boldsymbol{P}_I)^{-1} + \boldsymbol{H}\boldsymbol{P}(\boldsymbol{S}_I\boldsymbol{F}_D - \boldsymbol{Y}_I\boldsymbol{\lambda}_I)(\boldsymbol{H}\boldsymbol{P}_I)^{-1} + (\boldsymbol{X}_{0\infty}\boldsymbol{H}\boldsymbol{P}\boldsymbol{Y}_I - \boldsymbol{X}_{1\infty}\boldsymbol{H}\boldsymbol{P}\boldsymbol{S}_I)(\boldsymbol{H}\boldsymbol{P}_I)^{-1} + \frac{1}{Pe^2}[\boldsymbol{H}\boldsymbol{P}_I\boldsymbol{F}_D^{\sharp}(\boldsymbol{H}\boldsymbol{P}_I)^{-1} + \boldsymbol{H}\boldsymbol{P}\boldsymbol{S}_I^{\sharp}(\boldsymbol{H}\boldsymbol{P}_I)^{-1}\boldsymbol{X}_{0\infty} - \boldsymbol{X}_{0\infty}\boldsymbol{H}\boldsymbol{P}\boldsymbol{S}_I^{\sharp}(\boldsymbol{H}\boldsymbol{P}_I)^{-1}] \tag{47}$$

Table 3. Long-Time Asymptotic Values of $192\left(X_{2\infty} - \frac{1}{Pe^2}\right)$

K''	Approx. by Radial Collocation $n=2$	$n=3$	$n=4$	Analytic Values*
0	1.0	1.0	1.0	1.0
0.1	0.9947	1.0023	1.0023	1.0023
1.0	0.8751	0.9548	0.9549	0.9549
10.0	0.1893	0.4043	0.4096	0.4096
∞	0.0418	0.2302	0.2397	0.2397

*From Eq. 54 of Sankarasubramanian and Gill (1973–4) or Eq. 25 of DeGance and Johns (1978); the last value is from Aris (1980).

Here $\boldsymbol{\lambda}_I$ stands for diag $\{\lambda_1, \ldots \lambda_N\}$, and $\boldsymbol{P}_I$ consists of the first N columns of the model matrix $\boldsymbol{P}$. Thus $\boldsymbol{H}\boldsymbol{P}_I$ is a square matrix of order N, and is nonsingular since $\boldsymbol{H}$ and $\boldsymbol{P}_I$ have full rank. $\boldsymbol{F}_D$ and $\boldsymbol{F}_D^{\sharp}$ are diagonal matrices formed from the first N diagonal elements of $\boldsymbol{F}$ and $\boldsymbol{F}^{\sharp}$ in Eqs. 39 and 40. The nN by N matrices $\boldsymbol{S}_I$ and $\boldsymbol{Y}_I$ have the elements

$$S_{ij} = F_{ij}/(\lambda_j - \lambda_i), \qquad i \neq j \tag{48}$$

$$Y_{ij} = \frac{F_{ij}F_{jj}}{(\lambda_j - \lambda_i)^2} - \sum_{\substack{k=1 \\ k\neq j}}^{nN} \frac{F_{ik}F_{kj}}{(\lambda_j - \lambda_i)(\lambda_j - \lambda_k)}, \quad i \neq j \tag{49}$$

$$S_{ii} = Y_{ii} = 0 \tag{50}$$

The elements of $\boldsymbol{S}_I^{\sharp}$ are like those of $\boldsymbol{S}$, except that $\boldsymbol{F}^{\sharp}$ replaces $\boldsymbol{F}$. Finally, the diagonal matrix $(\boldsymbol{F}\boldsymbol{S})_D$ of order N contains the first N diagonal elements of $\boldsymbol{F}\boldsymbol{S}$.

Equations 45–47 show that the long-time dispersion coefficients $\boldsymbol{X}_{i\infty}$ are independent of the initial perturbation $\Gamma(\xi, Z)$. However, for multicomponent systems ($N > 1$) they depend on the chosen transverse weighting $\boldsymbol{W}(\xi)$, as predicted by Hatton (1981) and by DeGance and Johns (1985).

Calculated Dispersion Coefficients for Binary Reactive Systems

For binary systems, Eqs. 45–47 take the scalar forms

$$X_{0\infty} = \lambda_1 \tag{51}$$

$$X_{1\infty} = F_{11} \tag{52}$$

$$X_{2\infty} = \frac{1}{Pe^2} + \sum_{k=2}^{n} \frac{F_{1k}F_{k1}}{\lambda_1 - \lambda_k} \tag{53}$$

Table 4. Long-Time Limits of the Dispersion Coefficient Matrices X_i, Calculated with

$$Pe \to \infty,\ \boldsymbol{D} = \begin{bmatrix} 1.00 & 0.30 \\ -0.20 & 0.20 \end{bmatrix},\quad \boldsymbol{K}'' = \begin{bmatrix} 0.35 & 0.15 \\ -0.05 & 0.00 \end{bmatrix},\quad \text{and}\quad \boldsymbol{K}''' = \begin{bmatrix} 0.00 & 0.00 \\ 0.02 & 0.02 \end{bmatrix}$$

Collocation Order, n	Matrix $X_{0\infty}$		Matrix $X_{1\infty}$		Matrix $X_{2\infty}$	
2	−0.64074 + 000	−0.27288 + 000	0.52794 + 000	0.11123 − 001	0.37316 − 002	−0.61373 − 002
	0.72403 − 001	−0.22628 − 001	0.21812 − 002	0.50743 + 000	0.42334 − 002	0.20055 − 001
3	−0.64074 + 000	−0.27288 + 000	0.52796 + 000	0.11129 − 001	0.38283 − 002	−0.61177 − 002
	0.72403 − 001	−0.22628 − 001	0.21943 − 002	0.50744 + 000	0.44106 − 002	0.20245 − 001
4, 5, 6	−0.64074 + 000	−0.27288 + 000	0.52976 + 000	0.11129 − 001	0.38283 − 002	−0.61177 − 002
	0.72403 − 001	−0.22628 − 001	0.21943 − 002	0.50744 + 000	0.44108 − 002	0.20245 − 001

Table 5. Long-Time Limits of the Dispersion Coefficient Matrices X_i, Calculated with

$$Pe \to \infty,\ D = \begin{bmatrix} 1.00 & 0.30 \\ -0.20 & 0.20 \end{bmatrix},\quad K'' = \begin{bmatrix} 3.50 & 1.50 \\ -0.50 & 0.00 \end{bmatrix},\quad \text{and}\quad K''' = \begin{bmatrix} 0.00 & 0.00 \\ 0.20 & 0.20 \end{bmatrix}$$

Collocation Order, n	Matrix $X_{0\infty}$		Matrix $X_{1\infty}$		Matrix $X_{2\infty}$	
2	−0.34115 + 001	−0.13719 + 001	0.65139 + 000	0.47921 − 001	0.29964 − 002	−0.60397 − 002
	0.37929 + 000	−0.31494 + 000	0.37094 − 001	0.57571 + 000	−0.83677 − 003	0.16038 − 001
3	−0.34121 + 001	−0.13722 + 001	0.65058 + 000	0.47470 − 001	0.22358 − 002	−0.68046 − 002
	0.38632 + 000	−0.31164 + 000	0.49218 − 001	0.58154 + 000	0.30997 − 002	0.19009 − 001
4	−0.34121 + 001	−0.13722 + 001	0.65051 + 000	0.47436 − 001	0.21438 − 002	−0.68484 − 002
	0.38639 + 000	−0.31160 + 000	0.49490 − 001	0.58167 + 000	0.33754 − 002	0.19139 − 001
5, 6	−0.34121 + 001	−0.13722 + 001	0.65051 + 000	0.47436 − 001	0.21430 − 002	−0.68487 − 002
	0.38639 + 000	−0.31160 + 000	0.49492 − 001	0.58167 + 000	0.33780 − 002	0.19141 − 001

independent of the radial weighting. Here $-X_{0\infty}$ is the first-order decay rate of the remaining reactant mass in units of τ^{-1}, $X_{1\infty}$ is the mean velocity of this material relative to V_{max}, and $X_{2\infty}$ is its rate of longitudinal spreading, each quantity being a long-time limit.

Numerical comparisons of these collocation solutions with analytic values (Sankarasubramanian and Gill, 1973, 1974; DeGance and Johns, 1978; Aris, 1980) are shown in Tables 1–3. The collocation results converge rapidly with increasing n, and at $n = 4$ the accuracy of the rounded analytic values is reached.

The effects of chemical kinetics on the moments in Tables 1–3 are instructive. A homogeneous reaction with Damköhler number K''' alters only the moment $X_{0\infty}$, and does so in the obvious way (DeGance and Johns, 1980). A heterogeneous reaction alters $X_{0\infty}$ in the same direction, but to a limited extent because diffusion to the wall is necessary for the reaction. A heterogeneous reaction increases the pulse velocity $X_{1\infty}$ and reduces the spreading rate $X_{2\infty}$, by preferentially reducing the reactant concentration near the wall where the velocity is least and the velocity gradient is largest. The wall reaction effects have been interpreted similarly by Sankarasubramanian and Gill (1973) for their long-time dispersion coefficients $K_i(\infty)$.

Calculated Dispersion Coefficients for Multicomponent Reaction Systems

Tables 4, 5 and 6 show the dispersion-coefficient matrices in the long-time limit, for three multicomponent systems with non-simple matrices D, K'' and K'''. Axial molecular diffusion is neglected, i.e., the Pe^{-2} terms in Eq. 47 are suppressed. The kinetics for Table 4 are

$$\left.\begin{array}{ll} A \underset{0.15}{\overset{0.15}{\rightleftharpoons}} B \xrightarrow{0.05} C & \text{on the wall} \\ A \xrightarrow{0.02} C & \text{in the fluid} \end{array}\right\} \qquad (54)$$

and the kinetics for Tables 5 and 6 are 10 and 100 times faster. Species B and C are chosen for the basis, and the area average weighting $W(\xi) = I$ is used. The collocation method again converges well. No previous solutions are available for comparison.

The meanings of the multicomponent moments parallel those for binary systems. The matrix $-X_{0\infty}$ describes the total first-order decay toward the original equilibrium state, $-X_{1\infty}$ describes the mean velocities associated with the composition dis-

Table 6. Long-Time Limits of the Dispersion Coefficient Matrices X_i, Calculated with

$$Pe \to \infty,\ D = \begin{bmatrix} 1.00 & 0.30 \\ -0.20 & 0.20 \end{bmatrix},\quad K'' = \begin{bmatrix} 35.0 & 15.0 \\ -5.0 & 0.00 \end{bmatrix},\quad \text{and}\quad K''' = \begin{bmatrix} 0.00 & 0.00 \\ 2.00 & 2.00 \end{bmatrix}$$

Collocation Order, n	Matrix $X_{0\infty}$		Matrix $X_{1\infty}$		Matrix $X_{2\infty}$	
2	−0.54485 + 001	−0.17679 + 001	0.74412 + 000	0.96837 − 002	0.90943 − 003	−0.13420 − 002
	−0.98009 + 000	−0.28486 + 001	0.22424 − 001	0.72950 + 000	−0.84006 − 003	0.37320 − 002
3	−0.54357 + 001	−0.17623 + 001	0.74259 + 000	0.27919 − 002	0.14004 − 002	−0.29433 − 002
	−0.98263 + 000	−0.28484 + 001	0.51481 − 001	0.75366 + 000	0.10402 − 002	0.85281 − 002
4	−0.54356 + 001	−0.17623 + 001	0.74193 + 000	0.23970 − 002	0.98102 − 003	−0.32322 − 002
	−0.98264 + 000	−0.28484 + 001	0.52798 − 001	0.75443 + 000	0.19309 − 002	0.91059 − 002
5	−0.54356 + 001	−0.17623 + 001	0.74193 + 000	0.23943 − 002	0.97137 − 003	−0.32378 − 002
	−0.98264 + 000	−0.28484 + 001	0.52807 − 001	0.75444 + 000	0.19488 − 002	0.91162 − 002
6	−0.54356 + 001	−0.17623 + 001	0.74193 + 000	0.23943 − 002	0.97132 − 003	−0.32378 − 002
	−0.98264 + 000	−0.28484 + 001	0.52807 − 001	0.75444 + 000	0.19489 − 002	0.91162 − 002

turbance, and $-X_{2\infty}$ describes the covariance of the longitudinal displacements of the species.

Discussion

Orthogonal collocation is a simple way to handle the radial gradients in reactor problems. With $n = 1$ and $Pe \to \infty$, one obtains a generalized version of the plug flow model. With $n \geq 2$ and a radially varying velocity, convective dispersion is predicted. The number of radial nodes required depends on the steepness of the gradients, and is best determined by numerical convergence studies for the given problem as in Tables 4–6. The method is also readily set up for nonlinear problems, where numerical solution methods will normally be required.

Radially averaged models are awkward for catalytic reactor problems, because the dispersion coefficients depend nonlinearly on the surface kinetics. This dependence has been noted previously for binary systems (Sankarasubramanian and Gill, 1973, 1974; DeGance and Johns, 1978; Aris, 1980; Hatton and Lightfoot, 1984), and becomes very complicated in multicomponent systems as shown in Eqs. 45–47 and Tables 4–6. Note also that a solution for the concentration field or its moments M_i is required for each new problem before the dispersion coefficients can be calculated. We conclude that radial averaging, though useful for summarizing known results, is a questionable approach for predictive calculations.

Acknowledgment

This research was supported by Grants CPE-8308748 and CBT-8618571 from the National Science Foundation. We also thank the reviewers for their suggestions.

Notation

$\boldsymbol{B}''$ = matrix defined in Eq. 11, of order nN
$[\mathcal{D}]$ = diffusivity matrix, $m^2 \cdot s^{-1}$
$\mathcal{D}_{ref}$ = maximum absolute element of $[\mathcal{D}]$
$\boldsymbol{D}^{(N)} = [\mathcal{D}]/\mathcal{D}_{ref}$, dimensionless diffusivity matrix of order N
$\boldsymbol{D}$ = dimensionless block-diagonal diffusivity matrix in Eq. 11, of order nN
$\boldsymbol{F}, \boldsymbol{F}^{\#}$ = matrices defined in Eqs. 39 and 40
$\hat{G}$ = specific Gibbs energy, $J \cdot kg^{-1}$
$\boldsymbol{G}$ = Hessian of $\hat{G}$, Eq. B4
$I_n(x)$ = modified Bessel function of the first kind
$\boldsymbol{I}$ = identity matrix
$\boldsymbol{K}''$ = dimensionless coefficient matrix for heterogeneous production rates, $\boldsymbol{R}\boldsymbol{k}''/\mathcal{D}_{ref}$
$\boldsymbol{K}'''$ = dimensionless coefficient matrix for homogeneous production rates, $\boldsymbol{R}^2\boldsymbol{k}'''/\mathcal{D}_{ref}$
$\ell_j(\xi^2) = \prod_{\substack{k=1 \\ k \neq j}}^{n+1} (\xi^2 - \xi_k^2)/(\xi_j^2 - \xi_k^2)$, Lagrange interpolation polynomial
$\boldsymbol{M}_i, \boldsymbol{m}_i$ = longitudinal moment vectors defined in Eqs. 28 and 42
N = number of linearly independent variables $\Delta\omega_i$
n = number of interior collocation points ξ_i
$\boldsymbol{P}$ = matrix of column eigenvectors of $\boldsymbol{B}''$
p = parameter in Fourier transform $\bar{\Omega}$
$Pe = RV_{max}/\mathcal{D}_{ref}$, Peclet number
R = wall radius, m
t = time, s
$V(\xi)$ = dimensionless axial velocity, unity at centerline
V_{max} = centerline velocity, $m \cdot s^{-1}$
$\boldsymbol{V}$ = dimensionless velocity matrix in Eq. 11, of order nN
w_i = Gaussian integration weights
$W(\xi)$ = radial weight function in Eq. 41
$\boldsymbol{X}_i$ = dimensionless dispersion coefficient matrices in Eq. 41
$\boldsymbol{X}_{i\infty}$ = long-time limit of $\boldsymbol{X}_i$
$Z = z\mathcal{D}_{ref}/V_{max}R^2$, dimensionless axial coordinate
z = axial coordinate, m

Greek letters

$\boldsymbol{\Gamma}(\xi, Z)$ = initial disturbance profile in Eq. 4
$\boldsymbol{\lambda} = \boldsymbol{P}^{-1}\boldsymbol{D}\boldsymbol{P}$, diagonal array of eigenvalues of $\boldsymbol{B}''$, in descending order
λ_i = ith eigenvalue in $\boldsymbol{\lambda}$
ξ = dimensionless radial coordinate, unity at wall
τ = dimensionless time, $t\mathcal{D}_{ref}/R^2$
$\boldsymbol{\Omega}$ = collocation state vector defined in Eq. 10
$\bar{\boldsymbol{\Omega}} = \int_{-\infty}^{\infty} e^{-p\tau}\boldsymbol{\Omega}(\tau, Z)\, d\tau$, Fourier transform of $\boldsymbol{\Omega}$
$\Delta\boldsymbol{\omega}$ = mass-fraction displacement vector with independent elements $\Delta\omega_1, \ldots \Delta\omega_N$
$\Delta\boldsymbol{\omega}_\infty$ = solution for $\Delta\boldsymbol{\omega}$ at $Pe \to \infty$
$\Delta\tilde{\boldsymbol{\omega}}$ = collocation approximation to $\Delta\boldsymbol{\omega}$

Other symbols

$\langle f \rangle$ = area average of f over flow cross-section
iff = if and only if
$\boldsymbol{u}^T$ = transpose of vector or matrix $\boldsymbol{u}$

Literature Cited

Aris, R., "On the Dispersion of a Solute in a Fluid Flowing Through a Tube," *Proc. Roy. Soc. A*, **235,** 67 (1956).

Aris, R., "Hierarchies of Models in Reactive Systems," *Dynamics and Modelling of Reactive Systems*, W. E. Stewart, W. H. Ray, and C. C. Conley, eds., Academic Press, New York (1980).

Campbell, G. A., and R. M. Foster, *Fourier Integrals for Practical Applications*, D. Van Nostrand, Princeton, NJ (1967).

Casimir, H. B. G., "On Onsager's Principle of Microscopic Reversibility," *Rev. Mod. Phys.*, **17,** 343 (1945).

DeGance, A. E., and L. E. Johns, "The Theory of Dispersion of Chemically Active Solutes in a Rectilinear Flow Field," *Appl. Sci. Res.*, **34,** 189 (1978).

DeGance, A. E., and L. E. Johns, "On the Equivalence of Hermite and Power Moments in the Construction of Dispersion Approximations," *Chem. Eng. Sci.*, **34,** 1375 (1979).

DeGance, A. E., and L. E. Johns, "On the Construction of Dispersion Approximations to the Solution of the Convective Diffusion Equation," *AIChE J.*, **26,** 411 (1980).

DeGance, A. E., and L. E. Johns, "The Theory of Dispersion of Chemically Active Solutes in a Rectilinear Flow Field: The Vector Problem," *Appl. Sci. Res.*, **42,** 55 (1985).

DeGance, A. E., and L. E. Johns, "The Construction of Dispersion Approximations to the Solution of the Vector Convective Diffusion Equation," *Appl. Sci. Res.*, **43,** 239 (1987).

DeGroot, S. R., and P. Mazur, *Non-Equilibrium Thermodynamics*, North-Holland, Amsterdam (1962).

Gill, W. N., and R. Sankarasubramanian, "Exact Analysis of Unsteady Convective Diffusion," *Proc. Roy. Soc. A*, **316,** 341 (1970).

Hatton, T. A., "Convective Dispersion in Multiphase Contactors," Ph.D. Thesis, Univ. of Wisconsin-Madison (1981).

Hatton, T. A., and E. N. Lightfoot, "Dispersion, Mass Transfer and Chemical Reaction in Multiphase Contactors: I. Theoretical Developments," *AIChE J.*, **30,** 235 (1984).

Hindmarsh, A. C., and G. D. Byrne, "EPISODE: An Experimental Package for the Integration of Ordinary Differential Equations," Lawrence Livermore Laboratory Report UCID-30112 (1975).

Onsager, L., "Reciprocal Relations in Irreversible Processes, I, II," *Phys. Rev.*, **37,** 405 (1931); **38,** 2265 (1931).

Ramkrishna, D., and N. R. Amundson, *Linear Operator Methods in Chemical Engineering*, Prentice-Hall, Englewood Cliffs, NJ (1985).

Sankarasubramanian, R., and W. N. Gill, "Unsteady Convective Diffusion with Interphase Mass Transfer," *Proc. Roy. Soc. A*, **335,** 115 (1973); **341,** 407 (1974).

Stewart, W. E., "Simulation and Estimation by Orthogonal Collocation," *Chemical Engineering Education*, **XVIII,** 204 (Fall, 1984).

Taylor, G., "Dispersion of Soluble Matter in Solvent Flowing Slowly Through a Tube," *Proc. Roy. Soc. A*, **219,** 186 (1953).

Villadsen, J. V., and W. E. Stewart, "Solution of Boundary-Value Problems by Orthogonal Collocation," *Chem. Eng. Sci.*, **22**, 1483 (1967); **23**, 1515 (1968).
Villadsen, J. V., and M. L. Michelsen, *Solution of Differential Equation Models by Polynomial Approximation*, Prentice-Hall, Englewood Cliffs, NJ (1978).
Wang, J. C., "Collocation Modelling of Convective Dispersion," Ph.D. Thesis, Univ. of Wisconsin-Madison (1984).
AIChE J., **29**, 493 (1983).
Wang, J. C., "Collocation Modelling of Convective Dispersion," Ph.D. Thesis, Univ. Wisconsin-Madison (1984).

Manuscript received Apr. 12, 1988, and revision received Oct. 13, 1988.

Appendix A: Solution of Eqs. 30 and 31

The general solution of Eqs. 30 and 31 is:

$$\check{\boldsymbol{M}}_i = \exp(\lambda\tau)\check{\boldsymbol{M}}_i(0) + i\int_0^\tau \exp[\lambda(\tau - s)]\boldsymbol{P}^{-1}\boldsymbol{V}\boldsymbol{P}\check{\boldsymbol{M}}_{i-1}(s)\,ds + \frac{i(i-1)}{Pe^2}\int_0^\tau \exp[\lambda(\tau - s)]\boldsymbol{P}^{-1}\boldsymbol{D}\boldsymbol{P}\check{\boldsymbol{M}}_{i-2}\,ds, \quad \text{(A1)}$$

in which

$$\check{\boldsymbol{M}}_i = \boldsymbol{P}^{-1}\boldsymbol{M}_i. \quad \text{(A2)}$$

The solution is postulated in the form

$$\check{\boldsymbol{M}}_i = \sum_{r=0}^{i}\sum_{k=1}^{nN} \boldsymbol{a}_{kr}^{(i)}\tau^r \exp(\lambda_k\tau), \quad \text{(A3)}$$

consistent with Eqs. 32–40.

Suppose that the coefficient vectors $\boldsymbol{a}_{kr}^{(i-2)}$ and $\boldsymbol{a}_{kr}^{(i-1)}$ are known; then the values $\boldsymbol{a}_{kr}^{(i)}$ for $\check{\boldsymbol{M}}_i$ can be obtained by substituting Eq. A3 into Eq. A1. Thus, element m of the column vector $\boldsymbol{a}_{kr}^{(i)}$ is given by

$$a_{kr,m}^{(i)} = \check{M}_{i,m}(0) - i\sum_{r=0}^{i-1}\sum_{\substack{k=1\\k\neq m}}^{nN}(-1)^r \boldsymbol{F}_m\boldsymbol{a}_{kr}^{(i-1)}(r)!/(\lambda_k - \lambda_m)^{r+1} - \frac{i(i-1)}{Pe^2}\sum_{r=0}^{i-2}\sum_{\substack{k=1\\k\neq m}}^{nN}(-1)^r\frac{(r)!\boldsymbol{F}_m^{\#}\boldsymbol{a}_{kr}^{(i-2)}}{(\lambda_k - \lambda_m)^{r+1}}$$

$$\text{if} \quad k = m \quad \text{and} \quad r = 0 \quad \text{(A4)}$$

$$a_{kr,m}^{(i)} = i\boldsymbol{F}_m \cdot \boldsymbol{a}_{m,r-1}^{(i-1)}/r + \frac{i(i-1)}{Pe^2}\boldsymbol{F}_m^{\#}\boldsymbol{a}_{m,r-1}^{(i-2)}/r$$

$$\text{if} \quad k = m \quad \text{and} \quad 1 \le r \le i \quad \text{(A5)}$$

$$a_{kr,m}^{(i)} = i\sum_{j=r}^{i-1}(-1)^{j-r}\boldsymbol{F}_m\boldsymbol{a}_{kj}^{(i-1)}(j)!/[r!(\lambda_k - \lambda_m)^{j-r+1}] + \frac{i(i-1)}{Pe^2}\sum_{j=r}^{i-2}(-1)^{j-r}\boldsymbol{F}_m^{\#}\boldsymbol{a}_{kj}^{(i-2)}(j)!/[r!(\lambda_k - \lambda_m)^{j-r+1}]$$

$$\text{if} \quad k \neq m \quad \text{and} \quad 0 \le r \le i-1 \quad \text{(A6)}$$

$$a_{kr,m}^{(i)} = 0 \qquad \text{if} \quad k \neq m \quad \text{and} \quad r = i \quad \text{(A7)}$$

Here the row vectors $\boldsymbol{F}_m$ and $\boldsymbol{F}_m^{\#}$ are the mth rows of $\boldsymbol{P}^{-1}\boldsymbol{V}\boldsymbol{P}$ and $\boldsymbol{P}^{-1}\boldsymbol{D}\boldsymbol{P}$ respectively. Recursive application of Eqs. A3–A7 gives the functions $\check{\boldsymbol{M}}_i(\tau)$ up to any order i, and premultiplication by $\boldsymbol{P}$ gives the corresponding moments $\boldsymbol{M}_i(\tau)$ in Eq. 28.

Appendix B: Eigenvalues and Matrix Properties

The operator

$$\boldsymbol{T}: = \{T, D(T)\} \quad \text{(B1)}$$

consisting of the operation

$$T = \boldsymbol{D}^{(N)}\frac{1}{\xi}\frac{d}{d\xi}\left(\xi\frac{d}{d\xi}\right) - \boldsymbol{K}''', \quad 0 < \xi < 1 \quad \text{(B2)}$$

and the domain

$$D(T) = \{\boldsymbol{u} \in \mathcal{H};\ T\boldsymbol{u} \in \mathcal{H};\ \frac{d\boldsymbol{u}}{d\xi} = \boldsymbol{0} \quad \text{at} \quad \xi = 0;\ \boldsymbol{D}\frac{d\boldsymbol{u}}{d\xi} + \boldsymbol{K}''\boldsymbol{u} = \boldsymbol{0} \quad \text{at} \quad \xi = 1\} \quad \text{(B3)}$$

arises when separation of variables is applied to the radially continuous moment problem which we approximated in Eq. 30. Here we show that a suitable choice of the Hilbert space $\mathcal{H}$ renders $\boldsymbol{T}$ self-adjoint and allows a simple determination of its range of eigenvalues.

Let the matrices $\boldsymbol{D}^{(N)}$, $\boldsymbol{K}''$ and $\boldsymbol{K}'''$ be evaluated at a state which is locally stable at constant temperature and pressure (e.g., the upstream state). For stability in this sense, it is necessary and sufficient that the N × N Hessian matrix

$$\boldsymbol{G}: = \left\{\frac{\partial^2\hat{G}}{\partial\omega_i\partial\omega_j}\right\}_{p,T} \quad \text{(B4)}$$

of the specific Gibbs energy $\hat{G}$ be positive definite. Linear nonequilibrium thermodynamics (DeGroot and Mazur, 1962; Wang, 1984) then gives the factorizations

$$\boldsymbol{D}^{(N)} = \boldsymbol{L}\boldsymbol{G};\ \boldsymbol{K}'' = \boldsymbol{R}''\boldsymbol{G};\ \boldsymbol{K}''' = \boldsymbol{R}'''\boldsymbol{G} \quad \text{(B5)}$$

in which $\boldsymbol{L}$, $\boldsymbol{R}''$ and $\boldsymbol{R}'''$ are measurable matrices. Onsager's reciprocal relations (Onsager, 1931; Casimir, 1945) require symmetry of $\boldsymbol{R}''$ and $\boldsymbol{R}'''$, and also of $\boldsymbol{L}$ in negligible magnetic fields. The second law of thermodynamics requires positive definiteness of $\boldsymbol{L}$, and positive semidefiniteness of $\boldsymbol{R}''$ and $\boldsymbol{R}'''$.

Motivated by these results, we choose $\mathcal{H}$ as the Hilbert space (Ramkrishna and Amundson, 1985) of functions $\boldsymbol{u}$ in $D(T)$ with bounded norm

$$\|\boldsymbol{u}\|_2 = \left[\int_0^1 \boldsymbol{u}^T\boldsymbol{G}\boldsymbol{u}\xi\,d\xi\right]^{1/2} < \infty \quad \text{(B6)}$$

and inner product

$$\langle\boldsymbol{u}, \boldsymbol{v}\rangle = \int_0^1 \boldsymbol{u}^T\boldsymbol{G}\boldsymbol{v}\xi\,d\xi \quad \text{(B7)}$$

for every pair of included functions. Evaluation of the inner products $\langle\boldsymbol{T}\boldsymbol{u}, \boldsymbol{v}\rangle$ and $\langle\boldsymbol{u}, \boldsymbol{T}\boldsymbol{v}\rangle$ then gives the identity

$$\langle \boldsymbol{Tu}, \boldsymbol{v} \rangle = -\boldsymbol{u}^T \boldsymbol{GR}'' \boldsymbol{Gv}|_{\xi=1} - \int_0^1 \frac{d\boldsymbol{u}^T}{d\xi} \boldsymbol{GLG} \frac{d\boldsymbol{v}}{d\xi} \xi \, d\xi - \int_0^1 \boldsymbol{u}^T \boldsymbol{GR}''' \boldsymbol{Gv} \xi \, d\xi = \langle \boldsymbol{u}, \boldsymbol{Tv} \rangle \tag{B8}$$

Hence, $\boldsymbol{T}$ is self-adjoint with respect to the product defined in Eq. B7, and its eigenvalues accordingly are real. Special forms of this result were obtained by DeGance and Johns (1978) for binary fluids, and by Hatton (1981) for multicomponent fluids with diagonal $\boldsymbol{D}$.

Setting $\boldsymbol{v} = \boldsymbol{u}$ in Eq. B8 gives

$$\langle \boldsymbol{Tu}, \boldsymbol{u} \rangle = -\boldsymbol{u}^T \boldsymbol{GR}'' \boldsymbol{Gu}|_{\xi=1} - \int_0^1 \frac{d\boldsymbol{u}^T}{d\xi} \boldsymbol{GLG} \frac{d\boldsymbol{u}}{d\xi} \xi \, d\xi - \int_0^1 \boldsymbol{u}^T \boldsymbol{GR}''' \boldsymbol{Gu} \xi \, d\xi \tag{B9}$$

From the indicated properties of $\boldsymbol{G}$, $\boldsymbol{R}''$, $\boldsymbol{R}'''$ and $\boldsymbol{L}$, it follows that $\boldsymbol{GR}''\boldsymbol{G}$ and $\boldsymbol{GR}'''\boldsymbol{G}$ are positive semidefinite, and that $\boldsymbol{GLG}$ is positive definite. Thus, each righthand term in Eq. B9 is nonpositive, and the term involving $\boldsymbol{GLG}$ is negative unless $\boldsymbol{u}$ is constant on the interval (0, 1) so $\langle \boldsymbol{Tu}, \boldsymbol{u} \rangle$ is nonpositive.

The nonpositivity of $\langle \boldsymbol{Tu}, \boldsymbol{u} \rangle$ assures nonpositivity of the eigenvalues of $\boldsymbol{T}$, since these are given by $\lambda_k = \langle \boldsymbol{Tu}_k, \boldsymbol{u}_k \rangle / \langle \boldsymbol{u}_k, \boldsymbol{u}_k \rangle$ for each eigenfunction $\boldsymbol{u}_k$. Zero is an eigenvalue if, and only if, there exists a nonzero constant vector $\boldsymbol{a}_k$ such that $\boldsymbol{K}''\boldsymbol{a}_k = \boldsymbol{K}''\boldsymbol{a}_k = \boldsymbol{0}$. Thus, $\boldsymbol{T}$ has nonpositive eigenvalues generally, and strictly negative eigenvalues if, and only if, the upstream state $\Delta\boldsymbol{w} = \boldsymbol{0}$ is the only equilibrium solution of the kinetic scheme.

Since the matrix $\boldsymbol{B}''$ in Eq. 30 is a discrete approximation to the operator $\boldsymbol{T}$ with polynomial basis functions, we expect its eigenvalues in Eqs. 32–38 likewise to be real and to satisfy the same nonpositivity conditions.

Equation B5 and the condition of positive definite $\boldsymbol{G}$ imply reversibility of all included reactions. In numerical work, the requested accuracy and the true values of $\boldsymbol{K}''$ and $\boldsymbol{K}'''$ will determine whether or not it is reasonable to neglect some of the reverse reactions.

The matrix $\boldsymbol{K}'' + \boldsymbol{A}_{n+1,n+1}\boldsymbol{D}^{(N)}$ in Eq. 9 can be written as $(\boldsymbol{R}'' + \boldsymbol{A}_{n+1,n+1}\boldsymbol{L})\boldsymbol{G}$ by use of Eq. B5. The weight $A_{n+1,n+1}$ is positive for all n, since $\ell_{n+1}(\xi^2)$ increases monotonely for $\xi^2 > \xi_n^2$. From this and the properties of R'', L, and G, it follows that the matrix $\boldsymbol{K}'' + \boldsymbol{A}_{n+1,n+1}\boldsymbol{D}^{(N)}$ at a locally stable state is a product of positive definite matrices, and thus has a unique inverse as assumed in Eq. 7.